First publ. in: Nanotechnology 20 (2009), 075601

The structure and optical properties of ZnO nanocrystals embedded in SiO_2 fabricated by radio-frequency sputtering

G Mayer[1], M Fonin[1], U Rüdiger[1], R Schneider[2], D Gerthsen[2], N Janßen[3] and R Bratschitsch[3]

[1] Fachbereich Physik, Universität Konstanz, D-78457 Konstanz, Germany
[2] Laboratorium für Elektronenmikroskopie, Universität Karlsruhe, D-76131 Karlsruhe, Germany
[3] Fachbereich Physik, Universität Konstanz and Center for Applied Photonics, D-78457 Konstanz, Germany

E-mail: gillian.mayer@uni-konstanz.de

Received 15 August 2008, in final form 10 October 2008
Published 26 January 2009

Abstract

Zinc oxide (ZnO) nanocrystals (NCs) with high crystalline quality were prepared via radio-frequency magnetron sputtering as a SiO_2/ZnO/SiO_2 trilayer on Si(100) and Al_2O_3(0001) substrates with an intermediate *in situ* annealing step. Transmission electron microscopy reveals a uniform dispersion of ZnO NCs in the amorphous SiO_2 matrix with typical sizes up to 16 nm with a larger fraction of smaller crystals. The size distribution analysis yields a mean grain size of 5 nm for small particles. Individual ZnO NCs show a well-defined hexagonal close packed wurtzite structure and lattice parameters close to those of bulk ZnO, confirming their high crystalline quality. Mapping of the Zn distribution by means of energy-filtered transmission electron microscopy reveals a strongly non-uniform distribution of Zn within the SiO_2 matrix, corroborating the chemical separation of ZnO NCs from surrounding SiO_2. Optical transmittance measurements confirm the findings of the electron microscopy analysis. The fabrication technique described opens up new possibilities in the preparation of ZnO NCs with high crystalline quality, including growth in monolithic optical cavities without intermediate *ex situ* fabrication steps.

(Some figures in this article are in colour only in the electronic version)

1. Introduction

Zinc oxide (ZnO) is a wide gap semiconductor with a broad range of applications in the field of optoelectronic devices, such as laser or light emitting diodes [1, 2]. ZnO quantum dots have attracted considerable attention as their spins are potential candidates for qubits in quantum information technology [3, 4]. As photons can mediate an effective coupling between spins in two quantum dots [5], ZnO quantum dots embedded into an optical cavity may be envisioned as spintronic devices working at room temperature. Such a system could be manipulated on a femtosecond timescale, avoiding slow electrical contacts.

Different preparation methods have been established to grow ZnO nanocrystals (NCs). The most widely spread technique is sol–gel synthesis [6–11] mainly based on the work of Spanhel *et al* [12] or Seelig *et al* [13]. Other wet chemical methods like flame spray pyrolysis [14] or controlled double-jet precipitation [15] have also been successfully implemented. However, wet chemical procedures require drying of the NCs, which may result in the formation of secondary phases due to the large numbers of hydroxyl groups [16]. This can be avoided by solid state reactions such as mechanochemical preparation [16] and ion implantation [17, 18]. Also sputtering is suitable as a solvent-free preparation method. Recently, the fabrication of ZnO NCs via sputtering from a special mosaic-like target has been demonstrated with the main focus on the optical properties of the prepared composite systems [19–21]. The implementation of ZnO NCs in spintronic applications

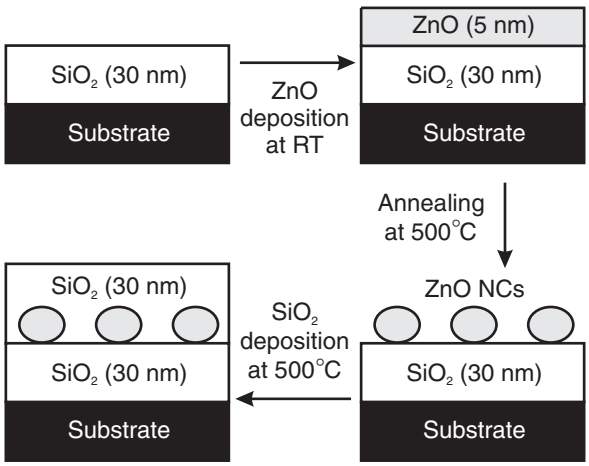

Figure 1. Schematic diagram illustrating the preparation process: after the deposition of a 5 nm thick ZnO layer on a 30 nm thick SiO_2 layer, the sample was annealed at 500 °C for 1 h. Subsequently, the 30 nm thick SiO_2 top layer was sputtered onto the hot sample.

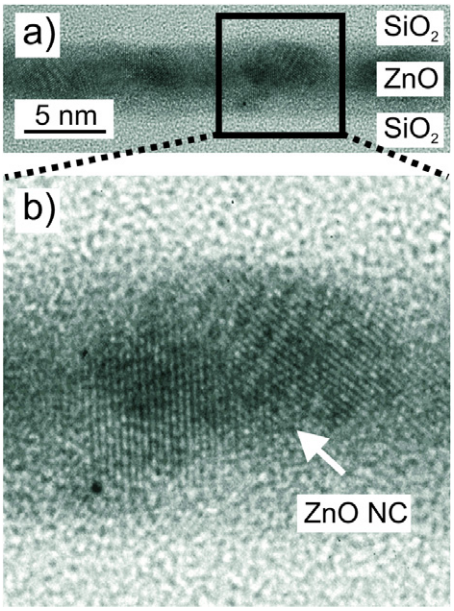

Figure 2. Structure of the ZnO layer embedded in SiO_2: (a) HRTEM image of the ZnO layer in cross-section, (b) magnification of a single ZnO NC.

requires long spin coherence times, which can be realized by embedding them into optical cavities [22]. Recently, a high-quality pillar microcavity operating in the ultraviolet has been fabricated by rf-magnetron sputtering of two Bragg mirrors with an intermediate layer containing colloidal ZnO quantum dots [23]. A disruption in the resonator fabrication process can be avoided by replacing colloidal quantum dots, which are spin coated outside the sputtering chamber, by their sputtered equivalents, forming a monolithic optical cavity without intermediate *ex situ* fabrication steps.

In this work, ZnO NCs with high crystalline quality embedded in a SiO_2 matrix were successfully prepared by radio-frequency (rf) magnetron sputtering. The crystalline quality of the ZnO NCs in SiO_2 was investigated in detail by means of transmission electron microscopy (TEM) focusing on the structural properties of distinct NCs. Additionally, optical transmittance measurements were performed on the ZnO/SiO_2 system confirming the findings of the electron microscopy analysis.

2. Experimental details

ZnO NCs in SiO_2 have been prepared by rf-magnetron sputtering of a SiO_2/ZnO/SiO_2 trilayer on Si(100) and Al_2O_3(0001) substrates. Figure 1 shows a schematic diagram of the preparation process. At the first preparation step a 30 nm thick SiO_2 layer was deposited onto Si(100) and Al_2O_3(0001) substrates at room temperature. A gas flow of 100 ml_n min^{-1} Ar and 8 ml_n min^{-1} O_2 was used. These preparation conditions lead to a working pressure of 4.5×10^{-3} mbar and a sputtering rate of about 0.7 Å s^{-1}. A ZnO film with a thickness of 5 nm was deposited onto the SiO_2 layer under the same conditions. After the deposition of ZnO the sample was annealed at 500 °C for 1 h. Subsequently, the SiO_2 top layer was deposited onto the hot sample, again with a gas flow of 100 ml_n min^{-1} Ar and 8 ml_n min^{-1} O_2.

Microstructural investigations of the ZnO layer sandwiched between the SiO_2 layers on Si(100) were performed by TEM using a Philips CM200 FEG/ST microscope at 200 kV acceleration voltage. The ZnO/SiO_2 composite system was imaged in cross-section and in plane-view using diffraction contrast, selected area electron diffraction (SAED) and high-resolution TEM (HRTEM). In addition, a 200 kV LEO 922 Omega microscope was used for imaging the element distribution by energy-filtered TEM (EFTEM) and for scanning TEM (STEM) imaging by means of a high-angle annular dark-field (HAADF) detector, yielding images with strong atomic number contrast (Z-contrast, see e.g. [24]). Standard TEM sample preparation techniques were used, including grinding, polishing to a thickness of about 10–20 μm, dimpling, and finally Ar^+-ion thinning. Optical measurements were performed at room temperature with an Agilent 8453E ultraviolet–visible spectrometer with a resolution of 1 nm.

3. Results and discussion

In order to study the microscopic structure of the prepared ZnO/SiO_2 composite system, detailed investigations were performed by TEM. Figure 2(a) shows a representative cross-section HRTEM image of the approximately 5 nm thick ZnO layer sandwiched between two SiO_2 layers. Slightly elongated ZnO NCs (dark regions) dispersed within the amorphous SiO_2 surrounding (bright background) are clearly discernable. A magnification of a typical inclusion is shown in figure 2(b) confirming the high crystalline quality of the prepared ZnO NCs. However, cross-section HRTEM images alone do not give a direct hint for the formation of separated ZnO NCs.

To verify this assumption and to enhance the contrast, plane-view TEM imaging was performed. The bright-field image shown in figure 3(a) suggests the presence of distinct ZnO NCs surrounded by SiO_2. EFTEM imaging visualizes

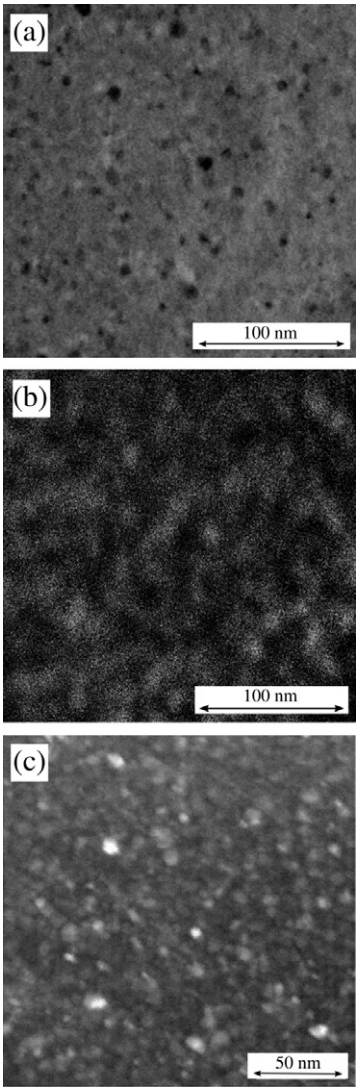

Figure 3. (a) Plane-view bright-field TEM image of the composite system, (b) corresponding EFTEM image of the Zn distribution and (c) HAADF STEM image.

a strongly inhomogeneous Zn distribution, hinting at the presence of regions highly enriched with ZnO. Figure 3(b) shows a representative chemical distribution map that was recorded in plane-view by the three-window technique [25] using the Zn $L_{2,3}$ ionization edge (threshold energy of 1020 eV). In this image local bright–dark contrast fluctuations with an extension of approximately 15–20 nm can be seen, where the bright regions have a higher Zn content. As the signal of inelastically scattered electrons decreases exponentially with the energy loss, the signal to noise ratio is low. Thus the regions enriched with Zn mapped with the high energy Zn $L_{2,3}$ edge at 1020 eV appear broadened in comparison to the TEM image. EFTEM directly provides a chemical distribution map of the sample. Figure 3(c) shows a representative HAADF STEM image of a plane-view specimen, where the regions with ZnO NCs appear brighter than the intermediate SiO_2 ones due to the higher mean atomic number. Thus, Z-contrast STEM imaging also shows a strongly inhomogeneous dispersion of Zn in the SiO_2 matrix, confirming the presence of areas enriched with ZnO. From these TEM measurements the ZnO-containing regions are estimated to be up to 16 nm in size.

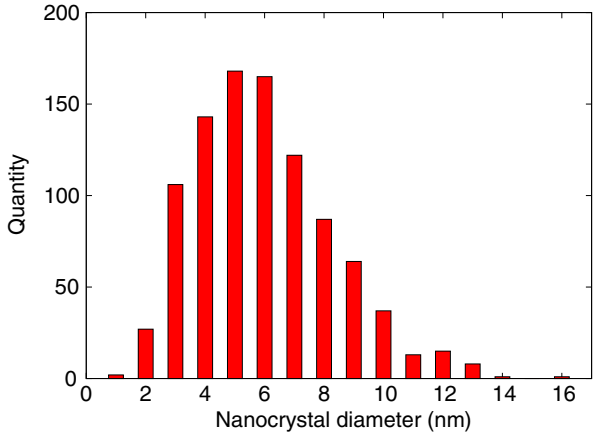

Figure 4. Size distribution of ZnO NCs.

To obtain a size distribution of the NCs, several TEM images were used and about 1000 NCs counted and measured in diameter. Figure 4 shows the resulting histogram. The distribution reveals that 73.4% of the NCs are 5 ± 2 nm in diameter. Only 3% of the NCs are smaller than 3 nm, 24.6% of the NCs are larger than 7 nm. The number of ZnO NCs with a diameter of less than 3 nm might be underrepresented in the histogram due to the limited resolution of the large area TEM images.

Figure 5(a) shows a SAED pattern of the ZnO/SiO_2 composite system taken from a plane-view sample with 200 kV electron acceleration voltage. A radial intensity profile of this pattern (figure 5(b)) reveals clear diffraction peaks which can be indexed by comparison with a simulated powder diffraction diagram of the ZnO wurtzite structure, where the reciprocal lattice vector k can be translated into a diffraction angle θ by applying the Bragg equation $2d_{\mathrm{rec}} \sin\theta = \lambda$ [26]. $d_{\mathrm{rec}} = \frac{2\pi}{k}$ denotes the reciprocal lattice constant and λ the wavelength of the incident beam. For 200 keV electrons the de Broglie wavelength λ equals 2.7424 pm. The mean grain size D of the NCs may be calculated from figure 5(b) by using the Scherrer formula

$$D = \frac{0.9\lambda}{\mathrm{FWHM}\cos\theta}$$

with FWHM representing the full width at half maximum (in radians) of the investigated diffraction peak. This formula is well known from x-ray diffraction (XRD) [26], but may also be applied to electron diffraction [27]. Especially the strong and well separated reflections (110), (103) and (112), and also (100), (002) and (101) at low diffraction angles may be used for the evaluation of D and lead to $D = 5 \pm 1$ nm. This is in good agreement with the results obtained from the TEM image analysis (see figure 4). As only small NCs broaden the FWHM of the diffraction peaks significantly, mainly their mean grain size is investigated with the radial intensity profile. The peaks are also somewhat broadened by image correction, as the SAED raw data is originally not entirely ring-shaped

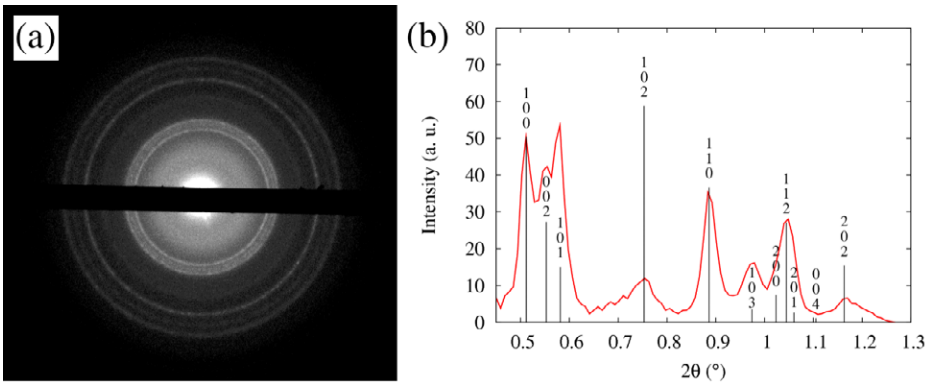

Figure 5. (a) SAED pattern of the ZnO/SiO_2 composite system and (b) comparison of a radial intensity profile of (a) (solid line) with a simulated powder diffraction diagram (indexed bars).

but slightly elliptic. Hence, the diffraction peaks may appear broader and so the NCs may appear smaller than the real size. The mean grain size of 5 nm fits well with the results of Ma *et al* [19] obtained by XRD for NCs which were, like our samples, annealed at 500 °C. The diffraction measurements may also be used for the estimation of the lattice constants, yielding $a = 3.24$ Å and $c = 5.20$ Å. The results are in good agreement with the values for bulk ZnO of $a = 3.25$ Å and $c = 5.21$ Å [28], and slightly closer to the bulk values than the parameters observed by HRTEM for a single ZnO NC prepared by the filtered cathodic vacuum arc technique, which yields $a = 3.17$ Å and $c = 5.17$ Å [29].

HRTEM imaging confirms the presence of crystalline, predominantly small ZnO NCs with sizes up to 16 nm, embedded in amorphous SiO_2. These sizes are in agreement with the results obtained by SAED, because not only large NCs of 16 nm in diameter but also many smaller NCs with a diameter less than or equal to 5 nm were found. In figure 6(a) an image of a typical ZnO NC with a diameter of about 10 nm is presented. The fast Fourier transform pattern (figure 6(b)) of the HRTEM image shows clear reflections up to the second order. For some orientations even the third order reflection is visible. The indexed diffraction pattern simulated with JEMS software [30] for the [001]-beam direction (figure 6(c)) confirms the wurtzite structure for the analyzed ZnO NC. From the HRTEM image in figure 6(a) a lattice constant of $a = 3.24$ Å is derived, which is consistent with the SAED result. Considering the measurement accuracy, this is again in good agreement with the ZnO bulk value of $a = 3.25$ Å [28]. High-resolution TEM imaging on different NCs reveals a structural anisotropy regarding the distribution of the hexagonal c-axis of ZnO NCs compared to the growth direction.

Optical transmittance measurements of ZnO NCs embedded in SiO_2 on $Al_2O_3(0001)$ yield information about the bandgap of the semiconductor sample. Figure 7 shows $(\alpha h\nu)^2$ as a function of photon energy $h\nu$, calculated from the optical transmittance spectrum, where α denotes the absorption coefficient. ZnO-related absorption sets in above 3.5 eV. A bandgap shift to higher energies due to quantum-confinement effects as observed for zero-dimensional quantum dots [31] is not observed here. In the high absorbance region, the models proposed by Tauc [32] and David *et al* [33] can be applied [34]. Then α depends on the photon energy $h\nu$ via $\alpha = C/(h\nu) \cdot \sqrt{h\nu - E_g}$, with C constant and E_g the direct bandgap. Following this relation, the bandgap is obtained by extrapolating the linear part of $(\alpha h\nu)^2$ to the $h\nu$ axis and estimated to be about 3.23 eV, as indicated by the dashed line (linear regression) in figure 7. However, the quantitative estimation of the bandgap is difficult in this case, as the absorption caused by ZnO is small due to the extremely thin ZnO layer. Thus, the edges of the range which can be used for extrapolation are not well-defined, which leads to a large variation of the

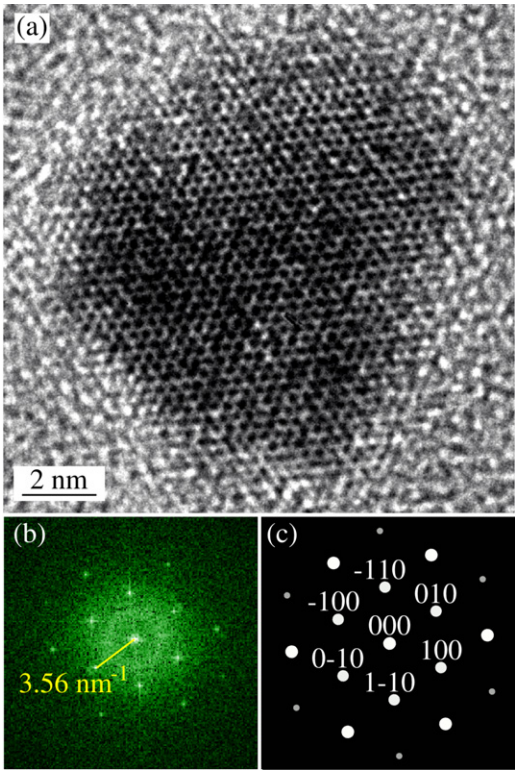

Figure 6. (a) Plane-view HRTEM micrograph of an individual ZnO NC surrounded by SiO_2, (b) fast Fourier transform of (a) showing hexagonal ZnO lattice reflection indices, (c) the corresponding simulated electron diffraction pattern for ZnO in the [001] orientation.

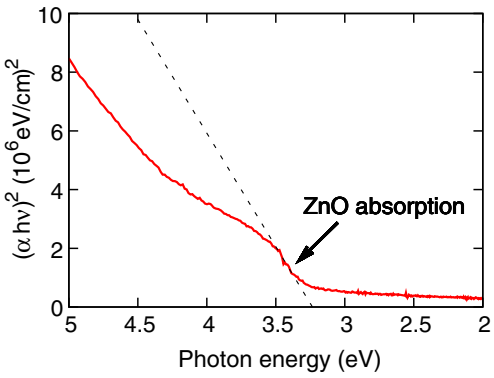

Figure 7. $(\alpha h\nu)^2$ value as a function of photon energy measured on the sample containing ZnO NCs.

bandgap depending on the choice of the edges. The bandgap as well as the size of ZnO NCs prepared in this study agree well with the values found by Tan *et al* [34] in NC-embedded ZnO thin films, which were annealed at 500 °C in a mixed O_2 and N_2 atmosphere. In contrast to SAED the large NCs dominate the optical transmittance spectra: in this study, the bandgap of bulk ZnO was observed because the NCs that are larger than 5 nm in diameter appear as bulk material, which has an energetically lower bandgap compared to smaller NCs. Consequently, their absorption emerges at lower energies, masking the absorption of smaller NCs.

Finally, we would like to demonstrate that our ZnO NC preparation method differs from others in an important way: we show that ZnO NCs in the amorphous SiO_2 matrix, sputtered as a layer structure, may be formed without a high temperature (>800 °C) annealing step. Such an annealing step was used by several groups to prepare ZnO NCs based on layer deposition [35, 29, 36]. However, Ma *et al* [19] reported that annealing at temperatures higher than 800 °C may easily lead to the formation of zinc silicate (Zn_2SiO_4) due to the large number of surface atoms of ZnO NCs and thus a high surface free energy to enable interface reactions. We also observed the formation of Zn_2SiO_4 at post annealing temperatures which were higher than 750 °C (not shown), which is in good agreement with the results found in [19]. Moreover, future optical cavities with embedded NCs will most likely be adversely affected, since interdiffusion of the different Bragg mirror materials might occur. Ma *et al* as well as Peng *et al* [20, 21, 37] deposited via rf-sputtering, but, in contrast to us, with a special mosaic-like target to perform co-sputtering of ZnO and SiO_2 (target attached sputtering). We suppose that the annealing step in the preparation in combination with the amorphous SiO_2 layer causes the ZnO layer to crack and form the NCs, which are then protected by the second SiO_2 layer, without formation of any mixed phases.

4. Conclusions

In summary, we have prepared ZnO NCs with high crystalline quality by rf-magnetron sputtering and investigated their structural and optical properties by means of TEM and optical transmittance. High-resolution TEM reveals a uniform dispersion of predominantly small ZnO NCs with sizes up to 16 nm. Individual ZnO NCs show a well-defined hcp wurtzite structure. Mapping of the Zn distribution by means of EFTEM reveals the strong non-uniform distribution of Zn within the SiO_2 matrix corroborating the chemical separation of ZnO NCs from surrounding SiO_2. SAED patterns confirm the wurtzite structure and together with the TEM image analysis indicate a mean grain size of about 5 nm for smaller NCs. Consistent with the size distribution, optical transmittance spectra reveal the bulk ZnO bandgap as large NCs dominate the spectra. The fabrication technique described opens up new possibilities in the preparation of ZnO NCs with high crystalline quality. Monolithic optical cavities containing ZnO NCs may be grown without intermediate *ex situ* fabrication steps.

Acknowledgments

We thank for financial support the Kompetenznetz Funktionelle Nanostrukturen der Landesstiftung Baden-Württemberg (Project C 10) and the Center for Applied Photonics (Spintronics in an Optical Cavity, Project 03). This work was also supported by the Deutsche Forschungsgemeinschaft (DFG) through the priority program SPP 1285 (Project 8). RB acknowledges the support of the Center for Junior Research Fellows of the University of Konstanz.

References

[1] Aoki T, Hatanaka Y and Look D C 2000 ZnO diode fabricated by excimer-laser doping *Appl. Phys. Lett.* **76** 3257
[2] Mandalapu L J, Yang Z, Chu S and Liu L J 2008 Ultraviolet emission from Sb-doped p-type ZnO based heterojunction light-emitting diodes *Appl. Phys. Lett.* **92** 122101
[3] Loss D and DiVincenzo D P 1998 Quantum computation with quantum dots *Phys. Rev.* A **57** 120
[4] Janßen N, Whitaker K M, Gamelin D R and Bratschitsch R 2008 Ultrafast spin dynamics in colloidal ZnO quantum dots *Nano Lett.* **8** 1991
[5] Imamoğlu A, Awschalom D D, Burkard G, DiVincenzo D P, Loss D, Sherwin M and Small A 1999 Quantum information processing using quantum dot spins and cavity QED *Phys. Rev. Lett.* **83** 4204
[6] Meulenkamp E A 1998 Synthesis and growth of ZnO nanoparticles *J. Phys. Chem.* B **102** 5566
[7] Volbers N, Zhou H, Knies C, Pfisterer D, Sann J, Hofmann D M and Meyer B K 2007 Synthesis and characterization of ZnO:Co^{2+} nanoparticles *Appl. Phys.* A **88** 153
[8] Ray S C *et al* 2007 Size dependence of the electronic structures and electron–phonon coupling in ZnO quantum dots *Appl. Phys. Lett.* **91** 262101
[9] Cheng H M, Lin K F, Hsu H C, Lin C J, Lin L J and Hsieh W F 2005 Enhanced resonant raman scattering and electron–phonon coupling from self-assembled secondary ZnO nanoparticles *J. Phys. Chem.* B **109** 18385
[10] Lin K F, Cheng H M, Hsu H C, Lin L J and Hsieh W F 2005 Band gap variation of size-controlled ZnO quantum dots synthesized by solgel method *Chem. Phys. Lett.* **409** 208
[11] Schwartz D A, Norberg N S, Nguyen Q P, Parker J M and Gamelin D R 2003 Magnetic quantum dots: synthesis, spectroscopy, and magnetism of Co^{2+}- and Ni^{2+}-doped ZnO nanocrystals *J. Am. Chem. Soc.* **125** 13205
[12] Spanhel L and Anderson M A 1991 Semiconductor clusters in the sol–gel process: quantized aggregation, gelation, and

crystal growth in concentrated zinc oxide colloids *J. Am. Chem. Soc.* **113** 2826
[13] Seelig E W, Tang B, Yamilov A, Cao H and Chang R P H 2003 Direct synthesis of ZnO nanoparticles by a solution-free mechanochemical reaction *Mater. Chem. Phys.* **80** 257
[14] Mädler L, Stark J W and Pratsinis S E 2002 Rapid synthesis of stable ZnO quantum dots *J. Appl. Phys.* **92** 6537
[15] Zhong Q and Matijević E 1996 Preparation of uniform ZnO colloids by controlled double-jet precipitation *J. Mater. Chem.* **6** 443
[16] Shen L, Bao N, Yanagisawa K, Domen K, Gupta A and Grimes C A 2006 Direct synthesis of ZnO nanoparticles by a solution-free mechanochemical reaction *Nanotechnology* **17** 5117
[17] Amekura H, Umeda N, Sakuma Y, Kishimoto N and Buchal C 2005 Fabrication of ZnO nanoparticles in SiO_2 by ion implantation combined with thermal oxidation *Appl. Phys. Lett.* **87** 013109
[18] Liu Y X, Liu Y C, Shen D Z, Zhong G Z, Fan X W, Kong X G, Mu R and Henderson D O 2002 The structure and photoluminescence of ZnO films prepared by post-thermal annealing zinc-implanted silica *J. Cryst. Growth* **240** 152
[19] Ma J G, Liu Y C, Xu C S, Liu Y X, Shao C L, Xu H Y, Zhang J Y, Lu Y M, Shen D Z and Fan X W 2005 Preparation and characterization of ZnO particles embedded in SiO_2 matrix by reactive magnetron sputtering *J. Appl. Phys.* **97** 103509
[20] Peng Y Y, Hsieh T E and Hsu C H 2006 Optical characteristics and microstructure of ZnO quantum dots–SiO_2 nanocomposite films prepared by sputtering methods *Appl. Phys. Lett.* **89** 211909
[21] Peng Y Y, Hsieh T E and Hsu C H 2006 White-light emitting ZnO–SiO_2 nanocomposite thin films prepared by the target-attached sputtering method *Nanotechnology* **17** 174
[22] Ghosh S, Wang W H, Mendoza F M, Myers R C, Li X, Samarth N, Gossard A C and Awschalom D D 2006 Enhancement of spin coherence using q-factor engineering in semiconductor microdisc lasers *Nat. Mater.* **5** 261
[23] Thomay T *et al* 2008 Colloidal ZnO quantum dots in ultraviolet pillar microcavities *Opt. Express* **16** 9791
[24] Crewe A V 1984 An introduction to the STEM *J. Ultrastruct. Res.* **88** 94
[25] Egerton R F 1996 *Electron Energy Loss Spectroscopy in the Electron Microscope* (New York: Plenum)
[26] Cullity B D and Stock S R 2001 *Elements of X-Ray Diffraction* 3rd edn (Upper Saddle River, NJ: Prentice-Hall)
[27] Oprea C, Ciupina V and Prodan G 2008 Investigation of nanocrystals using TEM micrographs and electron diffraction technique *Rom. J. Phys.* **53** 223
[28] Abrahams S C and Bernstein J L 1969 Remeasurement of the structure of hexygonal ZnO *Acta Crystallogr.* B **25** 1233
[29] Zhang X H, Chua S J, Yong A M and Chow S Y 2006 Exciton radiative lifetime in ZnO quantum dots embedded in SiO_x matrix *Appl. Phys. Lett.* **88** 221903
[30] Stadelmann P A 1987 EMS—a software package for electron diffraction analysis and HREM image simulation in materials science *Ultramiscroscopy* **21** 131
[31] Nakamura A, Okamatsu K, Tawara T, Gotoh H, Temmyo J and Matsui Y 2008 Dot-height dependence of photoluminescence from ZnO quantum dots *Japan. J. Appl. Phys.* **47** 3007
[32] Tauc J 1970 *Amorphous and Liquid Semiconductors* (London: Plenum)
[33] David E A and Mott N F 1970 Conduction in non-crystalline systems v. conductivity, optical absorption and photoconductivity in amorphous semiconductors *Phil. Mag.* **22** 903
[34] Tan S T, Chen B J, Sun X W, Fan W J, Kwok H S, Zhang X H and Chua S J 2005 Blueshift of optical band gap in ZnO thin films grown by metal-organic chemical-vapor deposition *J. Appl. Phys.* **98** 013505
[35] Kim S, Kim C O, Hwang S W and Choi S H 2008 Growth and enhanced light emission of hybrid structures of ZnO/Si nanocrystals *Appl. Phys. Lett.* **92** 243108
[36] Kim K K, Koguchi N, Ok Y W, Seong T Y and Park S J 2004 Fabrication of ZnO quantum dots embedded in an amorphous oxide layer *Appl. Phys. Lett.* **84** 3810
[37] Peng Y Y, Hsieh T E and Hsu C H 2007 Dielectric confinement effect in ZnO quantum dots embedded in amorphous SiO_2 matrix *J. Phys. D: Appl. Phys.* **40** 6071